Available online at www.sciencedirect.com
ScienceDirect
Thermochimica Acta 449 (2006) 42–46
thermochimica acta
www.elsevier.com/locate/tca

# A kinetic study of the thermal degradation of ammonium species inside a 3D zincophosphate

Djordje Stojakovic[a,*], Nevenka Rajic[a], Natasa Zabukovec Logar[b], Venceslav Kaucic[b]

[a] Faculty of Technology and Metallurgy, University of Belgrade, 11000 Belgrade, Serbia
[b] National Institute of Chemistry, Hajdrihova 19, 1000 Ljubljana, Slovenia

Received 9 June 2006; received in revised form 20 July 2006; accepted 23 July 2006

## Abstract

Ammonium ions remain inside the 3D zincophosphate framework after the hydrothermal crystallization. These species in co-operation with sodium cations exert a specific templating role in the formation of the open-framework lattice. The decomposition of the ammonium species under non-isothermal conditions has been studied by the non-parametric kinetics (NPK) method. The process is characterized by a complex kinetic mechanism and a relatively high activation energy for the main reaction step, $E_a = 336$ kJ/mol. These reflect the fact that the decomposition of the ammonium ions inside the zincophosphate framework involves not only the diffusion of the liberated species through the narrow channels of the microporous framework but also a prior overcoming of strong electrostatic interactions and the breaking of hydrogen bonds.

*Keywords:* NPK method; Non-isothermal kinetics; Open-framework; TG; 3D zinc phosphate; Hydrothermal synthesis

## 1. Introduction

Open-framework metal phosphates have been intensively investigated owing to their versatile structural chemistry and widespread application in the fields of catalysis, molecular adsorption, ion exchange and important technologies such as electronics and optoelectronics. Mostly, the three-dimensional structures display nanosized regular and accessible cages and channels, which enables open-framework phosphates to act as nanoreactors, also allowing only molecules of appropriate shapes and size to enter the pores [1–3].

The formation of these compounds is usually structure-directed by organic amines, which stay in the interlayer area interacting with inorganic host through hydrogen bonds and van der Waals interactions. A thermal treatment (calcination) is necessary to remove organic species and to leave the lattice accessible for application. However, the guest–host interactions are sometimes so strong that their breaking affects the skeleton.

In this work we investigate the interactions of ammonium cations with the 3D zincophosphate framework. This system has been chosen for at least two reasons: (1) during calcination only ammonium species leave the framework and (2) the position of these ions is crystallographically determined. Thermal analysis therefore seems to be quite an appropriate method for studying the interactions of ammonium ions with the framework. The analysis has included a kinetic study of the thermal degradation of ammonium species inside the porous framework.

## 2. Experimental

### 2.1. Synthesis

Zincophosphate (ZnPO) was prepared from a mixture of $Zn(NO_3)_2$, $(NH_4)_2HPO_4$ and disodium salt of terephthalic acid. These components were mixed with water in a molar ratio of 1:1:1:200, respectively, and heated in a Teflon-lined stainless steel autoclave at 220 °C for 24 h. The solid crystalline product was recovered by decantation and washing with distilled water. C, H, N analysis gave for N, 1.95 wt.% and for H, 0.54 wt.%, whereas elemental analysis obtained by inductively coupled plasma emission spectroscopy gave for Zn, 36.0 wt.% and for P, 17.0 wt.%. Since there are a lot of large prismatic colorless crystals present in the product, a suitable crystal was selected for the X-ray single crystal analysis.

---

* Corresponding author. Tel.: +381 11 3303 626; fax: +381 11 3370 387.
*E-mail address:* stojakovic@tmf.bg.ac.yu (D. Stojakovic).

0040-6031/$ – see front matter © 2006 Elsevier B.V. All rights reserved.
doi:10.1016/j.tca.2006.07.013

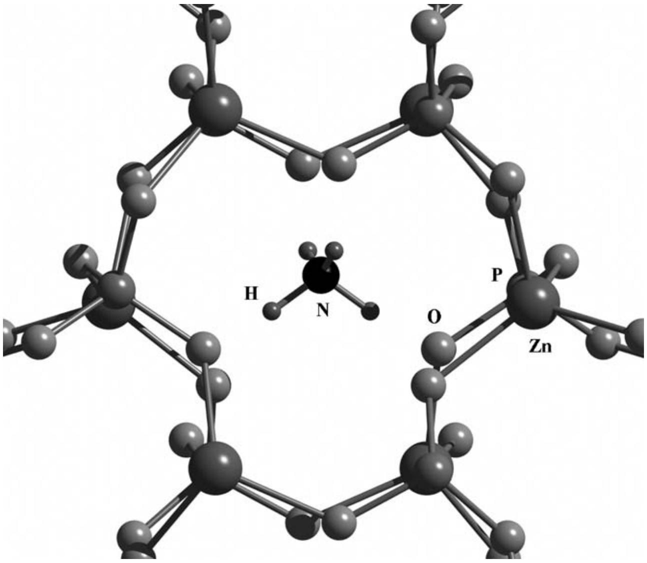

Fig. 1. Position of the $NH_4^+$ ion inside the channel of the ZnPO framework: view along the *a* crystallographic axis.

### 2.2. Instrumentation

Thermal decomposition was performed using a SDT Q-600 simultaneous DSC-TGA instrument (TA Instruments). The samples (mass approximately 10 mg) were heated in a standard alumina 90 μl sample pan. All experiments were carried out under nitrogen with a flow rate of 0.1 $dm^3$/min. Non-isothermal measurements were conducted at heating rates of 2, 5, 7, 10, 12 and 15 K/min. Five experiments were done at each heating rate.

## 3. Results and discussion

Unit cell determination from single crystal data collection showed that the obtained crystalline phase is $Na_{0.75}(NH_4)_{0.25}ZnPO_4$ [4], which is consistent with the elemental analyses. This also confirmed the fact that the bulk product is a single crystalline phase.

$Na_{0.75}(NH_4)_{0.25}ZnPO_4$ has been reported as having novel tetrahedral topology built from 3D network of $ZnO_4$ and $PO_4$ units connected via Zn–O–P links [4]. Two types of channels enclosed by six-membered ring[1] windows are occupied by the guest cations. The positions of $Na^+$ and $NH_4^+$ species are found to be different. It has been suggested that this particular combination of three smaller and one large univalent cation exerts co-templating effect leading to novel tetrahedral topology.

All $NH_4^+$ cations are found to be in only one type of channel, the geometry of which is more regular than for the other type [4]. The position of the cation is shown in Fig. 1. The cation forms four hydrogen bonds with the framework oxygen atoms: two of them having $d(H\cdots O) = 2.15$ Å and two having $d(H\cdots O) = 2.24$ Å (4). This indicates that in addition to being electrostatically bound to the framework, the cation is also rather strongly bound to the framework through hydrogen bonds. Fig. 2 shows the TG and DTG curves for $Na_{0.75}(NH_4)_{0.25}ZnPO_4$ in the 300–850 K range. It can be seen that the total weight loss amounts to only approximately 2.5 wt.% and it corresponds to the ammonium species decomposition.

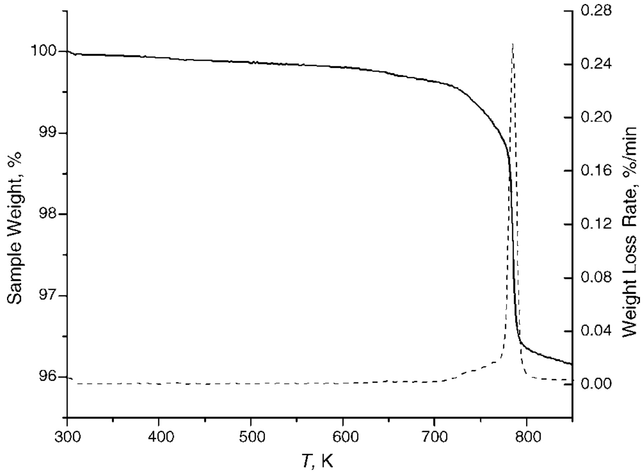

Fig. 2. TG/DTG curves for $Na_{0.75}(NH_4)_{0.25}ZnPO_4$ (TG, solid line; DTG, dot line).

### 3.1. Kinetics of the ammonium species decomposition during the thermal treatment of $Na_{0.75}(NH_4)_{0.25}ZnPO_4$

The ammonium species decomposition during the thermal treatment of $Na_{0.75}(NH_4)_{0.25}ZnPO_4$ has been studied in nitrogen atmosphere under non-isothermal conditions. The measurements have been carried out at six different heating rates: 2, 5, 7, 10, 12 and 15 K/min. Fig. 3 shows the corresponding $\alpha$ versus $T$ thermogravimetric curves ($\alpha$ is the conversion degree and $T$ is the absolute temperature), and Fig. 4 shows the corresponding $\beta\, d\alpha/dT$ versus $T$ ($\beta$ = heating rate) differential thermogravimetric curves.

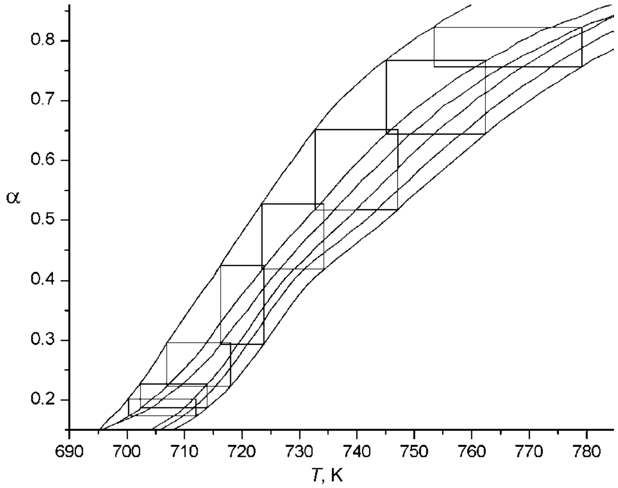

Fig. 3. Experimental curves for the $NH_4^+$ decomposition in $Na_{0.75}(NH_4)_{0.25}ZnPO_4$ at different heating rates (from left to right: 2, 5, 7, 10, 12 and 15 °C/min). The rectangles show the submatrices selected for the NPK analysis.

---

[1] The ring is defined by six tetrahedral atoms.

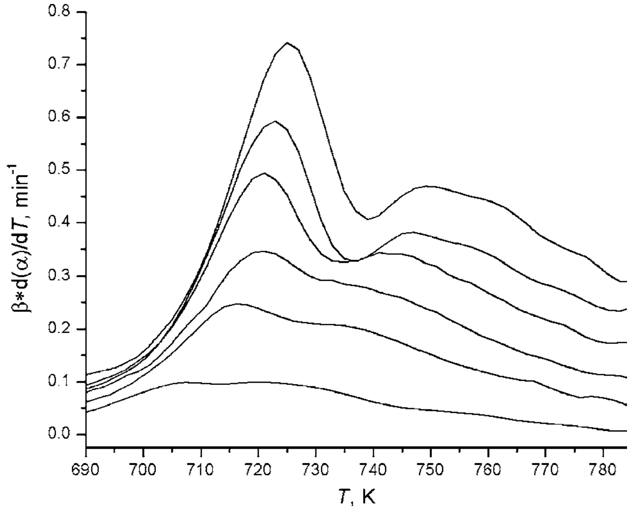

Fig. 4. Experimental reaction rates ($\text{min}^{-1}$) vs. temperature for the $NH_4^+$ decomposition in $Na_{0.75}(NH_4)_{0.25}ZnPO_4$ at different heating rates (from bottom to top: 2, 5, 7, 10, 12 and 15 °C/min).

The kinetics of the ammonium species decomposition has been studied by the non-parametric kinetics (NPK) method of Serra et al. [5–7]. This method for the analysis of non-isothermal thermogravimetrical data is based on the assumption that the reaction rate can be expressed as a product of two independent functions:

$$\text{Rate} = \frac{d\alpha}{dt} = f(\alpha)h(T) \tag{1}$$

where $f(\alpha)$ is the derivative form of the conversion function while the temperature-dependent function, $h(T)$, is usually the Arrhenius equation:

$$h(T) = k = A\ \exp\left(-\frac{E_a}{RT}\right)$$

The reaction rate, $d\alpha/dt$ ($d\alpha/dt = \beta\, d\alpha/dT$), measured from several experiments at different heating rates, can thus be expressed as a three-dimensional surface determined by the temperature and the conversion degree. This surface can be organized as an $(n \times m)$ matrix $\boldsymbol{A}$ where the rows correspond to different conversion degrees, from $\alpha_1$ to $\alpha_n$, while columns correspond to different temperatures, from $T_1$ to $T_m$.

The matrix $\boldsymbol{A}$ can be expressed as the product of two vectors:

$$\boldsymbol{A} = \boldsymbol{f}\boldsymbol{h}^{\mathrm{T}}$$

where

$$\boldsymbol{f}^{\mathrm{T}} = [f(\alpha_1)f(\alpha_2)f(\alpha_3)\cdots f(\alpha_n)]$$

$$\boldsymbol{h}^{\mathrm{T}} = [h(T_1)h(T_2)h(T_3)\cdots h(T_m)]$$

The NPK method uses the mathematical procedure known as the singular value decomposition (SVD) to decompose the matrix $\boldsymbol{A}$ and obtain the vectors $\boldsymbol{f}$ and $\boldsymbol{h}$. In this manner, the two functions in Eq. (1) can be decoupled without the need of any prior assumptions about their functionality. From the vectors $\boldsymbol{f}$ and $\boldsymbol{h}$, plots of $f(\alpha)$ against $\alpha$ and of $h(T)$ against $T$ are immediately available and the nature of the functions $f(\alpha)$ and $h(T)$ can be examined.

In actual practice it is not possible to experimentally obtain all the elements of the matrix $\boldsymbol{A}$ for a sufficient range of $\alpha$ values and temperatures. Recently, a multivariate regression technique has been applied to generate the matrix $\boldsymbol{A}$ [8–10]. However, some of the matrix elements that are obtained in this way are necessarily the result of extrapolation of the experimental data, whereas multivariate regression is generally applicable only for interpolation purposes.

Therefore, in this work the procedure as originally proposed by Serra et al. has been employed. It involves a subdivision of the $\alpha$ versus $T$ curves into partly overlapping submatrices. SVD is next applied on each submatrix; if $q$ submatrices were formed, SVD on each of them will yield $q$ matrices $\boldsymbol{U}_i$ and $\boldsymbol{V}_i$ as well as $q$ singular value vectors $\boldsymbol{s}_i$, respectively. The subdivision technique and the construction of continuous vectors $\boldsymbol{u}$ and $\boldsymbol{v}$ from the vectors $\boldsymbol{u}_i$ and $\boldsymbol{v}_i$ of individual matrices $\boldsymbol{U}_i$ and $\boldsymbol{V}_i$ are described in detail in refs. [6,11]. Furthermore, the subdivision procedure in this work has been amended by a variable step method in which the individual submatrices differ in size and shape (“adaptive NPK”) [12].

The above described treatment of the thermogravimetric data yielded 8 submatrices in the $\alpha$ range of 0.168–0.825 and the temperature range of 700–780 K (Fig. 3); a total of 40 different $\alpha$ values and 33 different temperatures has been used for the construction of the 8 submatrices. After SVD was applied on each submatrix, the resulting $\boldsymbol{s}_i$ vectors contained in all 8 cases one dominant value and two small values. In particular, for the first seven submatrices the dominant value in each individual $\boldsymbol{s}_i$ accounts for approximately 96% of the sum of values of that vector, whereas the other two values amount to approximately 3 and 0.7%, respectively. For the eighth submatrix (the top one in Fig. 3) the dominant value accounts for approximately 91%, and the other two for 6.4 and 2.3%, respectively. This indicates that in the 700–780 K range one predominant kinetic process (process 1) takes place, accompanied by two minor processes (processes 2 and 3).

The kinetic analysis for the process 1 proceeded as follows. From the vectors $\boldsymbol{u}_i$ and $\boldsymbol{v}_i$ of that process the vectors $\boldsymbol{u}_1$ and $\boldsymbol{v}_1$ were compiled, respectively. The results contained in the vector $\boldsymbol{u}_1$ are proportional to the function of conversion, $f(\alpha)$, and those in the vector $\boldsymbol{v}_1$ are proportional to the function of temperature, $h(T)$.

Fig. 5 shows the plot of the $f(\alpha)$ values from the compiled vector $\boldsymbol{u}_1$ versus $\alpha$. The values have been examined against various known kinetic models, but the vector $\boldsymbol{u}_1$ could not be satisfactorily fitted in most of them ($R^2$ of the fits being invariably <0.9). Only the Sestak–Berggren model [13] yielded reasonably acceptable fits. Its two-parameter form (2) gives a fit having $R^2 = 0.9932$, with the parameters $m = -0.39 \pm 0.01$ and $n = 3.56 \pm 0.09$. The three-parameter Sestak–Berggren Eq. (3) gives a fit having $R^2 = 0.9978$, with the parameters $m = -92.6 \pm 2$, $n = 47.6 \pm 0.8$ and $p = 92.3 \pm 2$. However, the produced values of the parameters do not seem to

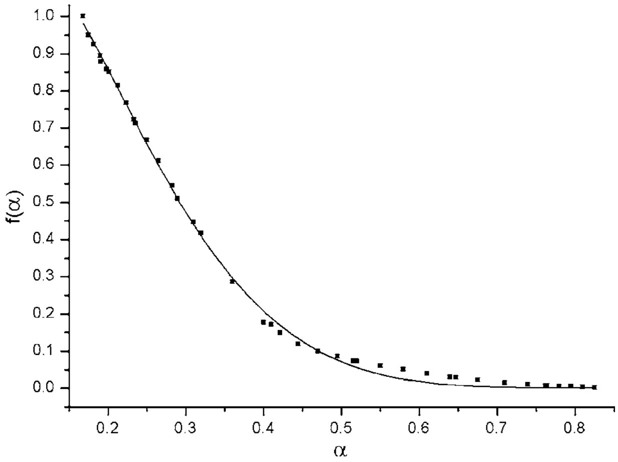

Fig. 5. A plot of *f*(*α*) [normalized within (0, 1)] vs. the degree of conversion: dark squares are the experimental points and the line is the fit obtained by Eq. (4).

convey any clear meaning.

$$f(\alpha) = \alpha^m (1-\alpha)^n \tag{2}$$

$$f(\alpha) = \alpha^m (1-\alpha)^n (-\ln(1-\alpha))^p \tag{3}$$

The best fit (the one shown in Fig. 5), although being only slightly better than for the Sestak–Berggren model, has been obtained with the following empirical expression ($R^2 = 0.9986$):

$$f(\alpha) = \frac{(1-\alpha)^m [-\ln(1-\alpha)]^n}{1-(1-\alpha)^p} \tag{4}$$

with $m = 7.13 \pm 0.4$, $n = 1.75 \pm 0.1$ and $p = 0.0776 \pm 0.02$.

The complexity of the kinetic mechanism is probably due to the fact that the decomposition of the ammonium species inside the phosphate framework involves not only an overcoming of strong electrostatic interactions between the cation and the anionic lattice, but also the rupture of strong hydrogen bonds and the diffusion of the liberated species through the comparatively narrow framework channels.

Fig. 6 shows the plot of the ln[*h*(*T*)] values from the compiled vector $\boldsymbol{v}_1$ versus 1/*T*. The slope of the straight line ($R = 0.990$) gives the activation energy as $E_a = 336 \pm 9$ kJ/mol. This relatively high activation energy reflects again the fact that ammonium ions are rather entrapped inside the cavities of the phosphate framework and it also indicates that the $NH_4^+$ ions are bound to the framework both by strong electrostatic interactions and by strong N–H···O hydrogen bonds. From the intercept, the value of $(4 \pm 3) \times 10^{22}\ \text{min}^{-1}$ is obtained and it essentially represents the Arrhenius pre-exponential constant *A*, somewhat modified by constants arising from scaling [11]. The obtained $E_a$ can be compared with the value (178 kJ/mol) found [14] for the thermal removal of cetyltrimethylammonium ion from the MCM-48 siliceous nanoporous material. While the cetyltrimethylammonium ion is obviously considerably bulkier than the $NH_4^+$ ion, it can not form hydrogen bonds with the MCM-48 framework. In addition, the latter material is of the mesoporous type and has larger pore openings than the microporous ZnPO lattice. These facts can account for the somewhat lower $E_a$ in MCM-48 than in $Na_{0.75}(NH_4)_{0.25}ZnPO_4$.

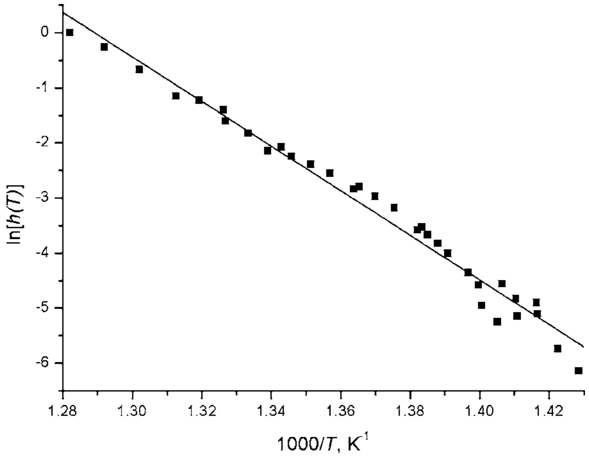

Fig. 6. An Arrhenius plot of ln[*h*(*T*)] vs. 1/*T*: dark squares are the experimental points and the straight line is the best fit.

The NPK analysis for the two minor processes (processes 2 and 3) can be carried out in analogous manner. That is, from the vectors $\boldsymbol{u}_i$ and $\boldsymbol{v}_i$ of the two processes the vectors $\boldsymbol{u}_2$ and $\boldsymbol{v}_2$, and the vectors $\boldsymbol{u}_3$ and $\boldsymbol{v}_3$ are compiled, respectively. However, the results contained in the obtained vectors $\boldsymbol{u}_2$, $\boldsymbol{v}_2$, $\boldsymbol{u}_3$ and $\boldsymbol{v}_3$ are quite scattered and the corresponding pairs of the *f*(*α*) versus *α*, and the ln[*h*(*T*)] versus 1/*T* plots do not give any smooth curves, thus preventing any further meaningful kinetic analysis of the two minor processes. Therefore, the results related to the processes 2 and 3 are not presented here. The cause of such scatter is probably twofold: firstly, the processes 2 and 3 contribute only slightly to the overall reaction rate; second, the entire ammonium ion decomposition is a process in which the mass of the sample is decreased by only 2.5%. These two facts cumulatively result in a rather low accuracy of the data for the two minor processes.

In order to obtain an independent confirmation of the complexity of the ammonium species decomposition during the thermal treatment of $Na_{0.75}(NH_4)_{0.25}ZnPO_4$, the model-free isoconversional method of Friedman [15] has been applied to the thermogravimetrical data. The method examines the dependence of $E_a$ upon *α*. If $E_a$ does not depend upon *α*, the kinetic process is simple and can be described by a unique “kinetic triplet” [$E_a$, *A*, *f*(*α*)] [16,17–20]. However, if $E_a$ significantly changes with *α*, the process is complex (multistep reaction).

The Friedman method uses the following form of the general rate expression:

$$\ln\left(b\frac{d\alpha}{dT}\right) = \ln A + \ln[f(\alpha)]\frac{E_a}{RT}$$

For $\alpha$ = constant, and using various heating rates (*b*), the plot of ln(*b*(d*α*/d*T*)) versus 1/*T* should be linear and from the slope of the straight line the value of $E_a$ can be obtained. Table 1 lists the results obtained when the Friedman method was applied to our data in the *α* range 0.2–0.8, together with the *R* values for each linear fit.

It is seen from Table 1 that $E_a$ varies considerably with the extent of conversion. These variations are an additional proof that the thermal decomposition of the ammonium species in $Na_{0.75}(NH_4)_{0.25}ZnPO_4$ is kinetically a multistep process.

Table 1
Activation energies at different degrees of conversion obtained by the Friedman method for the ammonium species decomposition during the thermal treatment of $Na_{0.75}(NH_4)_{0.25}ZnPO_4$

| $\alpha$ | $E_a$ (kJ/mol) | $R$ |
|---|---|---|
| 0.2 | 376 | 0.996 |
| 0.3 | 383 | 0.998 |
| 0.4 | 367 | 0.992 |
| 0.5 | 322 | 0.984 |
| 0.6 | 316 | 0.993 |
| 0.7 | 311 | 0.994 |
| 0.8 | 313 | 0.981 |

## 4. Conclusion

Ammonium species in co-operation with sodium cations exert a specific templating role in the formation of the open-framework ZnPO lattice during hydrothermal crystallization. The TG study has shown that the decomposition of the ammonium species in $Na_{0.75}(NH_4)_{0.25}ZnPO_4$ under non-isothermal conditions follows a rather complex kinetic mechanism. The activation energy for the main process is relatively high since the entrapped $NH_4^+$ species is bound quite strongly to the lattice both by electrostatic forces as well as by hydrogen bonds. The non-parametric kinetics method has proved fairly helpful in analyzing the process which involves a very small overall mass change (≈2.5%).

## Acknowledgements

This work was supported by the bilateral project “By rational synthesis towards smart materials” financed by the Serbian Ministry of Science and Environmental Protection and the Slovenian Ministry of Higher Education Science and Technology.

## References

[1] S. Coluccia, E. Gianotti, L. Marchese, Mater. Sci. Eng. 15 (2001) 219–229.
[2] Z.E. Lin, Q.X. Zeng, J. Zhang, G.Y. Yang, Microporous Mesoporous Mater. 64 (2003) 119–125.
[3] E. Coronado, E. Palomares, J. Mater. Chem. 15 (2005) 3593–3597.
[4] W.T.A. Harrison, Z. Kristallogr. 215 (2000) 288–292.
[5] R. Serra, R. Nomen, J. Sempere, J. Therm. Anal. Calorim. 52 (1998) 933–943.
[6] R. Serra, R. Nomen, J. Sempere, Thermochim. Acta 316 (1998) 37–45.
[7] J. Sempere, R. Nomen, R. Serra, J. Therm. Anal. Calorim. 56 (1999) 843–849.
[8] T. Vlase, G. Vlase, N. Doca, J. Therm. Anal. Calorim. 80 (2005) 207–210.
[9] T. Vlase, G. Vlase, A. Chiriac, N. Doca, J. Therm. Anal. Calorim. 80 (2005) 87–90.
[10] T. Vlase, G. Vlase, N. Doca, J. Therm. Anal. Calorim. 80 (2005) 425–433.
[11] J.D. Sewry, M.E. Brown, Thermochim. Acta 390 (2002) 217–225.
[12] J. Sempere, R. Nomen, R. Serra, J. Soravilla, Thermochim. Acta 388 (2002) 407–414.
[13] J. Sestak, G. Berggren, Thermochim. Acta 3 (1971) 1–12.
[14] M.J. Souza, A.O.S. Silva, J.M.F.B. Aquino, V.J. Fernandes Jr., A.S. Araujo, J. Therm. Anal. Calorim. 79 (2005) 493–497.
[15] H.L. Friedman, J. Polym. Sci. 6C (1965) 183–195.
[16] P. Budrugeac, C. Popescu, E. Segal, J. Therm. Anal. Calorim. 64 (2001) 821–827.
[17] P. Budrugeac, Polym. Degrad. Stabil. 89 (2005) 265–273.
[18] T. Vlase, G. Vlase, N. Doca, J. Therm. Anal. Calorim. 80 (2005) 425–428.
[19] M.E. Brown, M. Maciejewski, S. Vyazovkin, R. Nomen, J. Sempere, A. Burnham, J. Opfermann, R. Strey, H.L. Anderson, A. Kemmler, R. Keuleers, J. Janssens, H.O. Desseyn, C.-R. Li, T.B. Tang, B. Roduit, J. Malek, T. Mitsuhashi, Thermochim. Acta 355 (2000) 125–143.
[20] S. Vyazovkin, Thermochim. Acta 355 (2000) 155–163.